

High-dimensional Z' phenomenology at hadron colliders

Benjamin Fuks, Jochum J. van der Bij,^{*} and Qingjun Xu
*Physikalisches Institut, Albert-Ludwigs-Universität Freiburg,
Hermann-Herder-Straße 3, D-79104 Freiburg i.Br., Germany*
(Dated: November 11, 2018)

We study the phenomenology of a Z' -boson field coupled to hypercharge. The Z' propagator has a nontrivial Källén-Lehmann spectral density due to the mixing with a higher-dimensional inert vector field. As a consequence detection possibilities at hadron colliders are reduced. We determine the range of parameters where this field can be studied at the Tevatron and the LHC through its production cross section via the Drell-Yan mechanism.

I. INTRODUCTION

The present day data from high-energy colliders like LEP and Tevatron show that almost all measurements are described by the standard model at the loop level. Therefore extensions of the standard model tend to be strongly constrained. Typically such extensions will spoil the agreement with the data through a variety of effects, one of the most important of which is the appearance of flavor changing neutral currents. Even the most popular extension, the

Higgs mass [12, 14, 15, 16]. According to this point of view, measurements from LEP1 and SLD at the Z pole [17] were analyzed in Ref. [12], both for a four-dimensional and for the Heidi Z' models. The analysis on the technical level is not significantly different for the four-dimensional and the higher-dimensional case. The results of this analysis were recently confirmed in Ref. [14]. Fitting the data leads to constraints on the allowed parameter range of the Heidi models. We will restrict ourselves to the limits given in Ref. [12], which are on the conservative side.

The Drell-Yan-like production of a lepton pair at hadron colliders plays an important role in the present and future experimental program at the Fermilab Tevatron and CERN LHC colliders thanks to its large cross section and clean signature of the final state. This is also the primary discovery mode for additional neutral gauge bosons and has already been widely studied in the literature for the Tevatron and the LHC [18, 19, 20, 21, 22]. It has also been shown that the forward-backward asymmetry due to the interference between the three different exchange modes (γ , Z , and Z') could be an interesting observable [23, 24, 25, 26]. Therefore, in this work, we investigate for the first time the possible effects of a Heidi Z' on the Drell-Yan dilepton invariant-mass spectrum and the forward-backward asymmetry, both at the Tevatron and the LHC.

Because of the important theoretical uncertainties coming from QCD effects and missing large higher-order contributions, leading-order results for the Drell-Yan process, with or without additional Z' , are quite unreliable. A systematic approach to this problem is based on perturbation theory truncated at the next-to-leading order (NLO) [27, 28] or next-to-next-to-leading order [29] in the strong coupling constant α_s . In kinematical regions where higher-order contributions are enhanced due to the soft and collinear parton emission, soft-gluon resummation to all orders in α_s can be performed and matched with the fixed order predictions in order to improve the description of observables under consideration. However, a general procedure has not yet been developed and the resummation has to be done explicitly process by process. An alternative way of treating the soft-gluon emission is the parton shower, which approximates the full resummation calculation. However, the parton shower is universal for all processes and can be implemented easily in the analysis chains of the Tevatron and LHC experiments. Consequently, we implement in this work the Heidi Z' bosons in the Monte Carlo generator MC@NLO [30], generalizing the modified MC@NLO program including Z' gauge bosons inspired by grand unified theories of Ref. [20], which allows us to match NLO perturbative calculation with the parton shower of the Monte Carlo generator HERWIG [31] including color coherence effects and azimuthal correlations within and between jets. We subsequently compare the Monte Carlo predictions to the experimental results from the Tevatron for the invariant-mass spectrum and forward-backward asymmetry of the Drell-Yan production of lepton-pairs. In addition we study the sensitivity of the LHC experiments to the Heidi models for this channel.

The remaining part of the paper is organized as follows. In Sec. II we first describe the theoretical framework, i.e. the minimal Heidi Z' model, and discuss the implementation of Z' -boson production in the MC@NLO generator. Section III is devoted to the numerical analysis of the experimentally allowed Heidi parameter space and the investigation of the sensitivity of the LHC experiments to the model. Our conclusions are given in Sec. IV.

II. THEORETICAL FRAMEWORK

A. The minimal Heidi model

There is a large class of models containing extra neutral vector bosons [21, 22]. The simplest extension consists of the standard model plus one additional $U'(1)$ symmetry, the extended gauge group being $SU(3)_C \times SU(2)_L \times U(1)_Y \times U'(1)$.

We associate with the extra symmetry a \tilde{Z}'_μ field that is a singlet under the standard model gauge group. Moreover, we assume that no particle carries a $U'(1)$ charge. Therefore, this \tilde{Z}'_μ field is inert and its presence can only be noticed, because it can mix with the Abelian field \tilde{B}_μ associated with the $U(1)_Y$ symmetry. Because it does not couple to any fermions or Higgs fields, the additional \tilde{Z}'_μ field is allowed to move in D dimensions. As long as $D \leq 6$ the theory will stay renormalizable. In contrast, the \tilde{B}_μ field must be four-dimensional, because of its couplings to the fermionic fields. Therefore, in this basis, the hypercharge basis, we have two fields, a four-dimensional field coupled to the hypercharge and a higher-dimensional field coupled to nothing. However, the two fields can be mixed by a mass term. In order to describe the physics correctly, one has to transform to the mass basis. Allowing the $U(1)$ fields to have masses and mass-mixing terms, one finds for the gauge field part of the Lagrangian in the hypercharge basis [12]:

$$-\mathcal{L}_{\text{gauge}} = \frac{1}{4} \tilde{B}_{\mu\nu} \tilde{B}^{\mu\nu} + \frac{1}{2} m_4^2 \tilde{B}_\mu \tilde{B}^\mu + \frac{1}{4} \tilde{Z}'_{\mu\nu} \tilde{Z}'^{\mu\nu} + \frac{1}{2} m_D^2 \tilde{Z}'_\mu \tilde{Z}'^\mu + M_{\text{mix}}^{4-\frac{D}{2}} \tilde{Z}'_\mu \tilde{B}^\mu. \quad (1)$$

We have a four-dimensional mass m_4 , a higher-dimensional mass m_D , and a scale M_{mix} that connects the four-dimensional fields with the higher-dimensional ones. The two massive hypercharge fields Z'_μ and \tilde{B}_μ are transformed to the mass-eigenstates Z'_μ and B_μ , the latter being massless since the electromagnetic symmetry is exact. As a consequence, the three parameters m_4 , m_D , and M_{mix} are not independent and must satisfy the condition

$$\begin{cases} m_4^2 m_D^{6-D} = \mu_{\text{hd}}^{8-D} & \text{for } D \neq 6 \\ m_4^2 + \mu_{\text{hd}}^2 \ln \frac{m_D^2}{\mu_{\text{hd}}^2} = 0 & \text{for } D = 6 \end{cases}, \quad (2)$$

where we have introduced the quantity μ_{hd} in reference to the mixing of the low-dimensional and high-dimensional fields

$$\mu_{\text{hd}}^{8-D} \equiv \frac{\Gamma[3 - \frac{D}{2}]}{(4\pi)^{\frac{D}{2}-2}} M_{\text{mix}}^{8-D}. \quad (3)$$

By compactifying the higher dimensions and subsequently taking the continuum limit, one can derive the hypercharge-boson propagator which is of the form

$$D_{\mu\nu}^{\tilde{B}\tilde{B}}(q^2) = -ig_{\mu\nu} D^{\tilde{B}\tilde{B}}(q^2) = \begin{cases} -ig_{\mu\nu} \left[q^2 - m_4^2 + \mu_{\text{hd}}^{8-D} (q^2 - m_D^2)^{\frac{D-6}{2}} \right]^{-1} & \text{for } D \neq 6 \\ -ig_{\mu\nu} \left[q^2 - m_4^2 - \mu_{\text{hd}}^2 \ln \frac{m_D^2 - q^2}{\mu_{\text{hd}}^2} \right]^{-1} & \text{for } D = 6 \end{cases}, \quad (4)$$

and its nontrivial corresponding Källén-Lehmann spectral density

$$\rho(s) = -\frac{1}{2\pi i} \lim_{\varepsilon \rightarrow 0} \left[D^{\tilde{B}\tilde{B}}(s + i\varepsilon) - D^{\tilde{B}\tilde{B}}(s - i\varepsilon) \right], \quad (5)$$

which becomes in the four-, five- and six-dimensional cases

$$\begin{aligned} \rho_4(s) &= \frac{m_D^2}{m_D^2 + m_4^2} \delta(s) + \frac{m_4^2}{m_D^2 + m_4^2} \delta(s - m_D^2 - m_4^2), \\ \rho_5(s) &= \frac{2m_D^2}{2m_D^2 + m_4^2} \delta(s) + \frac{\theta(s - m_D^2)}{\pi} \frac{m_4^2 m_D (s - m_D^2)^{\frac{1}{2}}}{(s - m_4^2)^2 (s - m_D^2) + m_4^4 m_D^2}, \\ \rho_6(s) &= \frac{m_D^2}{m_D^2 + \mu_{\text{hd}}^2} \delta(s) + \theta(s - m_D^2) \frac{\mu_{\text{hd}}^2}{\left(s - \mu_{\text{hd}}^2 \ln \frac{s - m_D^2}{m_D^2} \right)^2 + \mu_{\text{hd}}^4 \pi^2}, \end{aligned} \quad (6)$$

respectively. For the three choices of the number of dimensions D , we recover models with one massless excitation which becomes the photon after the breaking of the electroweak symmetry. This is guaranteed by the condition of Eq. (2). However, while in the four-dimensional case we have a second peak corresponding to a massive resonance located at

$$m_{Z'}^2 \equiv m_D^2 + m_4^2, \quad (7)$$

for five- and six-dimensional singlet fields, we now have a massive continuum. As stated above, the presence of this new field affects the standard model Z -boson through a mixing which can be described by a quantity a_Y defined by [12]

$$\begin{aligned} a_{Y,4} &= \sin^2 \theta_W \frac{m_Z^2 m_4^2}{m_D^2 (m_4^2 + m_D^2)}, \\ a_{Y,5} &= \sin^2 \theta_W \int_{m_D^2}^{\infty} \frac{m_Z^2 ds}{2\pi m_D s} \frac{(2m_D^2 + m_4^2) m_4^2 (s - m_D^2)^{\frac{1}{2}}}{(s - m_D^2)^2 (s - m_4^2) + m_D^2 m_4^4}, \\ a_{Y,6} &= \sin^2 \theta_W \int_{m_D^2}^{\infty} m_Z^2 ds \frac{m_D^2 + \mu_{\text{hd}}^2}{m_D^2 s} \frac{\mu_{\text{hd}}^2}{\left[s - \mu_{\text{hd}}^2 \ln \frac{s - m_D^2}{m_D^2} \right]^2 + \pi^2 \mu_{\text{hd}}^4}, \end{aligned} \quad (8)$$

for the four-, five-, and six-dimensional cases, respectively. This quantity enters directly the vector and axial-vector coupling strengths of the Z boson to fermions, which read now

$$\begin{aligned} v_f &= e_f(\sin^2 \theta_W - a_Y) - \frac{1}{2}T_f^3(1 - a_Y) , \\ a_f &= -\frac{1}{2}T_f^3(1 - a_Y) . \end{aligned} \quad (9)$$

T_f^3 and e_f denote the weak isospin quantum number and the electric charge of the fermion f , and $\sin^2 \theta_W$ is the squared sine of the electroweak mixing angle. The coupling strengths of the new Z' state to fermion are simply given by the hypercharge

$$\begin{aligned} v'_f &= F(m_4, m_D) \sin \theta_W \left(\frac{T_f^3}{2} - e_f \right) , \\ a'_f &= F(m_4, m_D) \sin \theta_W \frac{T_f^3}{2} , \end{aligned} \quad (10)$$

with a prefactor F depending on the four-dimensional and high-dimensional masses.

One can interpret the propagator of Eq.(4) in two ways. The simplest way to treat the theory is to consider the field as a hypercharge gauge field with a nontrivial Källén-Lehmann spectral density. The other interpretation is to say that one has many (in this case a continuum of) single hypercharge coupled Z' fields, however, with a reduced coupling constant. The latter interpretation would be natural if we had an integer number of compact higher dimensions.

B. Heidi Z' production at hadron colliders

The Drell-Yan-like production of a lepton pair plays an important role in the present and future experimental program of hadron colliders thanks to its large cross section and clean signature of the final state. Since any observables related to this process are highly sensitive to the existence of an additional neutral gauge boson, this is their primary discovery mode. Following the conventions for the Drell-Yan process of Ref. [28], which are the ones used in the Monte Carlo generator MC@NLO, the corresponding squared matrix element reads

$$q\bar{q} \text{ or } qg \rightarrow \gamma, Z, Z' + X \rightarrow l^- l^+ + X, \quad (11)$$

and can be written as

$$\begin{aligned} |\overline{\mathcal{M}}_i|^2(q\bar{q} \text{ or } qg \rightarrow \gamma, Z, Z' \rightarrow l^- l^+ + X) &= \frac{1}{4} e^4 C_i \left\{ \frac{e_q^2}{M^4} T_i|_{1,0}^{1,0} \right. \\ &+ \frac{1}{\sin^4 \theta_W \cos^4 \theta_W} \frac{1}{(M^2 - m_Z^2)^2 + (\Gamma_Z m_Z)^2} T_i|_{A_q, B_q}^{A_l, B_l} \\ &+ \frac{1}{\sin^4 \theta_W \cos^4 \theta_W} \left| D^{\tilde{Z}' \tilde{Z}'}(M^2) \right|^2 T_i|_{A'_q, B'_q}^{A'_l, B'_l} \\ &- \frac{2e_q}{M^2} \frac{1}{\sin^2 \theta_W \cos^2 \theta_W} \frac{M^2 - m_Z^2}{(M^2 - m_Z^2)^2 + (\Gamma_Z m_Z)^2} T_i|_{v_q, a_q}^{v_l, a_l} \\ &- \frac{2e_q}{M^2} \frac{1}{\sin^2 \theta_W \cos^2 \theta_W} \text{Re} \left[D^{\tilde{Z}' \tilde{Z}'}(M^2) \right] T_i|_{v'_q, a'_q}^{v'_l, a'_l} \\ &+ \left. 2 \frac{1}{\sin^4 \theta_W \cos^4 \theta_W} \text{Re} \left[D^{\tilde{Z}' \tilde{Z}'}(M^2) \frac{(M^2 - m_Z^2) + i\Gamma_Z m_Z}{(M^2 - m_Z^2)^2 + (\Gamma_Z m_Z)^2} \right] T_i|_{v_q v'_q + a_q a'_q, v_q a'_q + v_q a'_q}^{v_l v'_l + a_l a'_l, v_l a'_l + v'_l a_l} \right\}, \quad (12) \end{aligned}$$

where M is the invariant-mass of the produced lepton pair, C_i is the corresponding color factor and the functions $T_i|_{A_q, B_q}^{A_l, B_l}$ depend on the kinematics of the process and on the order of the perturbative calculation. We have defined the coefficients

$$\begin{aligned} A_f^{(\prime)} &= a_f^{(\prime)2} + v_f^{(\prime)2}, \\ B_f^{(\prime)} &= 2a_f^{(\prime)} v_f^{(\prime)}, \end{aligned} \quad (13)$$

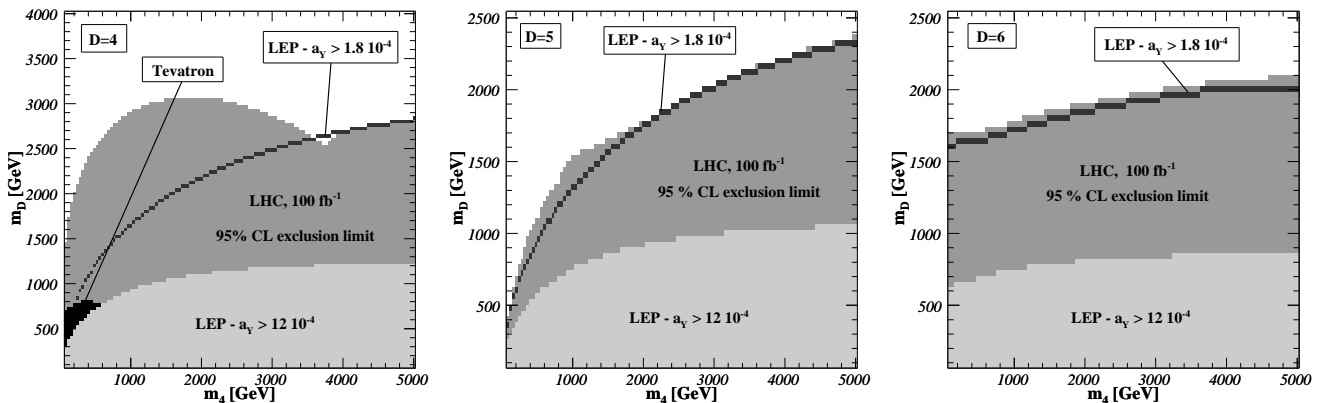


FIG. 1: The (m_4, m_D) plane for Heidi models with a four-dimensional (left), five-dimensional (center), and six-dimensional (right) Z' boson. We show the regions excluded by the LEP collider with (light gray region) and without (below the black line) leaving the forward-backward asymmetry of the bottom quarks, by the Tevatron (black region). We present also the region (dark gray) that the LHC experiments will be able to exclude at the 95% confidence level with an integrated luminosity of 100 fb^{-1} .

and a modified propagator $D^{\tilde{Z}'\tilde{Z}'}$ obtained by removing the photon and Z contributions from the propagator $D^{\tilde{B}\tilde{B}}$ of Eq. (4), since they have already been taken into account. The squared Z' -boson exchange as well as its interferences with the photon and Z -boson exchanges are included. We have adapted the MC@NLO program of Ref. [20] for the Drell-Yan process including Z' inspired by grand unified theories to the Heidi model case, which allow us to match the matrix elements of Eq. (12), describing correctly the hard parton emission by the initial state, to the HERWIG parton shower algorithm [31] describing the soft and collinear emission.

In the considered process, the incoming quark, antiquark, and gluon can give rise to an initial-state parton shower which is modeled in HERWIG by starting with the hard scattering partons and reconstructing backwards the preceding branchings. For a specific splitting of partons $i \rightarrow jk$, the energy fraction of parton j is distributed according to the LO DGLAP splitting functions and the phase space is restricted according to an angular ordered emission which is based on the Sudakov form factor. This allows us to sum the virtual corrections and unresolved real emissions to all orders and to correctly treat the infrared singularities. The parton shower stops when a cutoff scale defined by $(2.5\text{GeV})^2/E_i^2$ is reached, where a nonperturbative stage is imposed.

In order not to double count any contribution, the matching of the NLO matrix element to the parton shower achieved in MC@NLO uses two separate samples of Born-like and hard emission events which can have positive or negative weight. They are statistically distributed according to the positive-definite corresponding part of the NLO cross section and made separately finite by adding and subtracting the NLO part of the expanded Sudakov form factor [30]. The total cross section is then given by their weighted sum averaged over the total number of events.

III. ANALYSIS

A. Experimental constraints

Although there is no experimental evidence for the existence of a Z' boson, a number of data can be used to constrain the parameter space. For example, limits on the parameter a_Y , and thus indirectly on m_4 and m_D , can be obtained from precision measurements at the Z pole, strongly constraining the mixing between the standard model Z boson and the new field.

Regarding the limits from the LEP experiment there are two ways to proceed. One can take all the data from the precision measurements [17] and try to make a fit. The problem here is that the standard model is only barely compatible with these data due to the inconsistency of the forward-backward asymmetry A_{FB}^b of the bottom quarks with the rest of the data. Adding a Z' boson does not improve the situation, one finds a limit $a_Y \leq 1.8 \cdot 10^{-4}$ at the 95% confidence level. This problem with the data has led a number of authors to consider fitting the data leaving out A_{FB}^b [12, 14, 15, 16, 32, 33, 34]. In this case a good fit to the data is possible if a Z' boson is present [12, 14]. With a Higgs mass ranging from 115 to 495 GeV, a larger range of a_Y is allowed: $a_Y \leq 12 \cdot 10^{-4}$. As the situation is somewhat controversial we will present both limits in the following figures and discussions.

TABLE I: Heidi benchmark points accessible at the Tevatron and allowed by the LEP constraints after leaving out the forward-backward asymmetry of the bottom quarks.

	D	m_4 [GeV]	m_D [GeV]
A	5	100	300
B	6	50	650

Imposing these limits on minimal Heidi models with three free parameters, the number of dimensions D , the four-dimensional mass m_4 and the high-dimensional mass m_D , leads to the excluded regions shown in Fig. 1 for a four-dimensional (left), five-dimensional (center), and six-dimensional (right) additional neutral gauge boson. The light gray regions are the regions where $a_Y > 12 \cdot 10^{-4}$, while the dark line comes from the more stringent limits obtained by keeping all LEP data, i.e. it corresponds to $a_Y = 1.8 \cdot 10^{-4}$. The excluded regions are thus those below that line.

The best limits on the presence of a four-dimensional Z' boson come from the Tevatron collider. The principle guiding the search is straightforward. One uses the decay of the Z' boson into an electron-positron pair and looks for a peak in the invariant-mass. In addition one can use information on the forward-backward asymmetry of the leptons. One therefore needs a prediction for the Drell-Yan production cross section. Moreover, when one is working within a specific model, one can use the distribution of the leptons in the center-of-mass angle $\cos\theta^*$ with respect to the beam axis, leading to somewhat different limits for different models. This search has been made at the Tevatron [35] for the class of models discussed in Ref. [18], but not for the specific models presented here.

The model dependence is contained in the values of the vector and axial-vector coupling constants. As argued in Ref. [18] it would be useful to have lower limits on the mass of the Z' boson presented in the coupling constant plane. Unfortunately such a comparison has not been presented in the literature. Instead we estimate the lower limits for the allowed mass of the Z' -boson as a function m_4 and m_D , as follows. We use our implementation of the Heidi model in MC@NLO to predict the total cross section as a function of m_4 and m_D . Then, this cross section is normalized to the sequential Z' boson, which has a lower mass limit of $m_{Z'} = 923$ GeV [35]. We then connect the lower bounds on $m_{Z'}$ within the two studied models. The results are given in the dark area of Fig. 1 (left panel). The derived bounds are of course somewhat qualitative, because the sensitivity to the $\cos\theta^*$ distribution is not exactly modeled this way. A precise analysis would require taking into account a bidimensional distribution, including the angular one as well, whereby one cannot ignore detector effects [35]. However, this needs a detailed simulation of the detector and comparison with the actual data, which is beyond the scope of this paper.

For the higher-dimensional cases this procedure is not sufficient and a bin-by-bin comparison of predicted and measured Drell-Yan cross sections is needed. Unfortunately, these measurements are only presented in the literature [37] for a limited integrated luminosity. Within this limited statistics the Tevatron gives no improvement over the LEP data. However, we note that in Ref. [36] there appears to be an excess in the 300 – 400 GeV range, which might be consistent with a spread-out Z' boson. We hope that published numbers for the Drell-Yan cross section with a larger integrated luminosity will appear soon, so that these questions can be studied in more detail.

In Fig. 2, we compare our results with the limited statistics data published in Ref. [37]. We show both the differential cross section $d\sigma/dM$ and the forward-backward asymmetry. As an example, we chose the two Heidi benchmark points presented in Table I, which are just within the region of the parameter space allowed by the constraints coming from LEP, provided that the forward-backward asymmetry of the bottom quarks is left out, and “friendly” for the Tevatron. We show our predictions for the Heidi model together with those of the standard model, i.e. when no additional Z' boson is present. We use the CTEQ6M (NLO $\overline{\text{MS}}$) [38] sets for the parton densities in the proton and antiproton. As can be seen from the figures, all the predictions are compatible with the data for both observables. However, data with a higher luminosity would make it sensible to divide the studied invariant-mass range in smaller bins, which could be used to emphasize deviations from the standard model.

B. Predictions for the LHC

In this section, we discuss the sensitivity of the LHC experiments to Heidi models, considering four-dimensional, five-, and six-dimensional extra neutral gauge bosons. The discovery potential of the LHC is determined through the investigation of possible deviations from the standard model predictions in the tail of the Drell-Yan invariant-mass distribution, the studied range being

$$200 \text{ GeV} \leq M \leq 4500 \text{ GeV} . \quad (14)$$

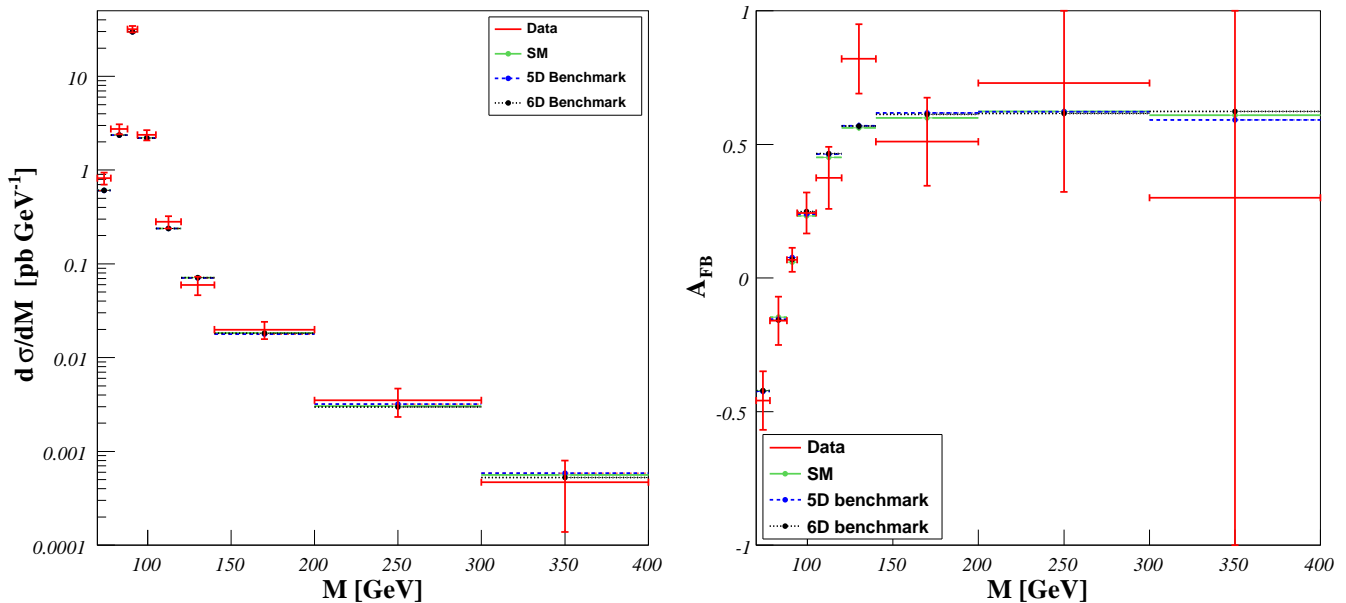


FIG. 2: Drell-Yan differential cross section and forward-backward asymmetry with and without Heidi Z' contributions at the Tevatron. The results are presented for the two benchmark points of Table I.

TABLE II: Typical Heidi benchmark points accessible at the LHC and allowed both by the Tevatron and by the LEP constraints, after leaving out the forward-backward asymmetry of the bottom quarks.

	D	m_A [GeV]	m_D [GeV]
C	4	500	300
D	5	200	400
E	6	50	700

The main source of background for Drell-Yan l^+l^- events is QCD multijet and direct photon production where the jets have a large electromagnetic component. However, with typical experimental selection cuts one can obtain a signal almost free from any QCD background, its part to the measurements being reduced to at most 1% [39, 40, 41]. For that reason, we apply the following cuts

$$\begin{cases} p_T > 20 \text{ GeV} \\ |\eta| < 2.5 \end{cases}, \quad (15)$$

to both leptons, which allows us to consider as a new physics signal any significant excess of l^+l^- events with respect to the standard model Drell-Yan irreducible background, neglecting thus any other source of background.

For each bin i of the investigated range of Eq. (14), we calculate the quantities N'_i and N_i , representing the number of events related to Drell-Yan-like lepton-pair production with and without an additional neutral gauge boson, respectively. For a given luminosity L , they can be derived from the differential cross section by

$$N_i^{(\prime)} = \int_{M_1}^{M_2} dM \frac{d\sigma^{(\prime)}}{dM} L, \quad (16)$$

where M_1 (M_2) is the lower (upper) limit of the considered bin, and $d\sigma$ ($d\sigma'$) the Drell-Yan cross section without (with) an additional Z' gauge boson. Expecting the standard model Drell-Yan background, we can estimate the significance of a possible Heidi signal through the quantity

$$\chi^2 = \sum_{i=1}^n \frac{(N_i - N'_i)^2}{N_i} \quad (17)$$

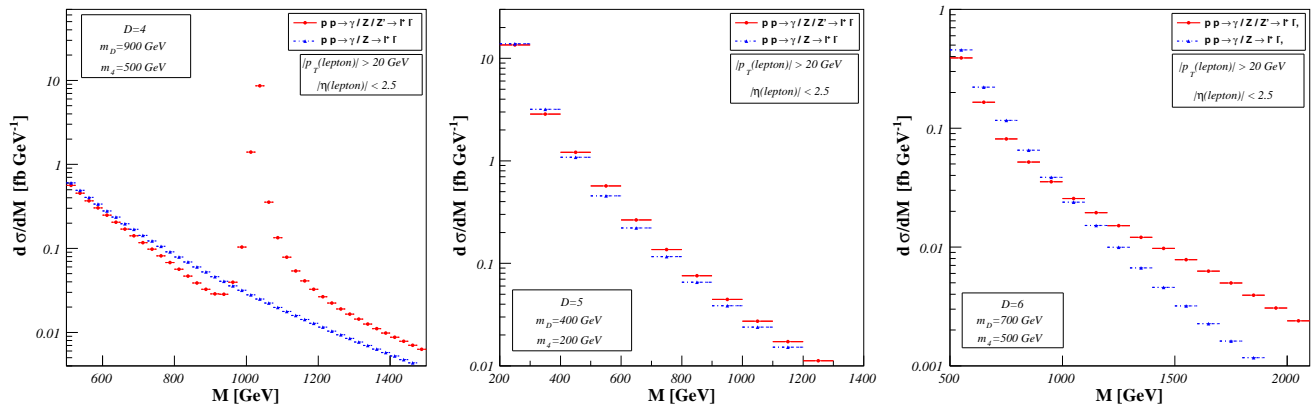


FIG. 3: Drell-Yan differential cross sections with (solid red) and without (dashed blue) additional Heidi Z' bosons at the LHC for the benchmark points presented in Table II. The typical experimental cuts of Eq. (15) are applied.

where n is the number of bins which the range of Eq. (14) is divided in. The LHC will then be able to exclude a given point of the Heidi parameter space at the 95% confidence level if the corresponding χ^2 is bigger than 21.

In order to take advantage of the differences between the standard model and the Heidi predicted line shape of the Drell-Yan mass spectrum in the high invariant-mass regions, we divide the studied range into nine bins of 100 GeV for $200 \text{ GeV} \leq M \leq 1100 \text{ GeV}$ and we take three larger bins at very high invariant-mass in order to have higher statistics, i.e. $1100 \text{ GeV} \leq M \leq 1300 \text{ GeV}$, $1300 \text{ GeV} \leq M \leq 1600 \text{ GeV}$, and $1600 \text{ GeV} \leq M \leq 4500 \text{ GeV}$. That allows us to avoid spurious sensitivities since we have then at least 50 expected events for each bin. This way we have a good idea of the typical reach of the LHC in the parameter space of the models. The results shown in Fig. 1 use cross sections calculated at a center-of-mass energy of 14 TeV with again the CTEQ6M (NLO $\overline{\text{MS}}$) [38] sets of parton densities, assuming a LHC luminosity of 100 fb^{-1} .

For the four-dimensional model, the LHC will be able to reach a mass range of several TeV, as can be seen from the dark gray region in the left panel of Fig. 1. This range can be divided in two areas, one at small value of m_4 and one at larger values. The first zone corresponds to a region where the Z' mass is smaller than or equal to about 3 TeV and is fairly typical since it is also found for other models with electroweak size couplings. In contrast, the LHC-reachable zone where m_4 is larger corresponds to a heavier Z' but with a much larger width due to the large value of the mixing parameter α_Y , which makes it possible to detect the new vector boson via its interferences with the standard model photon and Z boson. In comparison to the results of previous experiments, the LHC will allow us to considerably enlarge the model parameter space that can be investigated in the four-dimensional case. For the five-, and six-dimensional cases, however, the LHC will not be able to cover a parameter space region much larger than is already constrained by the LEP collider. This is the case if we take the strict limits that exist if we keep the data coming from the forward-backward asymmetry of the bottom quarks in the electroweak precision fit. As stated before, the resonance is replaced by a massive continuum, rendering the detection of any excess in the Drell-Yan distributions more complicated and restricting the regions of the parameter space that can be reached at the LHC, as can be seen in the central and right panels of Fig. 1. However, if one prefers to take the more conservative limits obtained by leaving out the forward-backward asymmetry of the bottom quarks, the LHC is sensitive to a range of parameters roughly double the size that is reached by previous colliders.

As an example, we show in Fig. 3 lepton-pair invariant-mass spectra for the benchmark points presented in Table II. We compare MC@NLO predictions including a Heidi Z' boson (solid red curves) with the ones expected in the standard model case (dashed blue curves). In the four-dimensional model (left panel of Fig. 3), far from the peak region located at the Z' mass given by Eq. (7), the spectra with and without Z' will of course coincide, while around the Z' mass, we have a clear resonance due to the presence of the extra field. For five-dimensional (central panel of Fig. 3) and six-dimensional (right panel of Fig. 3) extra neutral gauge bosons, the resonance is replaced by a massive continuum, which makes the detection a bit more tricky. However, large deviations can still easily be detected if we consider the line shapes of the distributions rather than the total number of events.

IV. CONCLUSIONS

We studied a new class of renormalizable models containing a Z' boson with a nontrivial Källén-Lehmann representation, derived from the mixing with an inert higher-dimensional field. Existing LEP limits constrain this class of models, but the amount depends on the interpretation of the analysis of the precision data, allowing for strict or loose limits. In the case of the loose limits we found, using a state of the art MC@NLO program, that the LHC will be able to study a large range of the allowed parameter space. In the case of the strict limits even the LHC will have difficulty to improve on existing bounds, but there may be some hope for a large luminosity option. Present bounds from the Tevatron, which may be relevant at low masses, are not satisfactory, since only a small fraction of the data have been analyzed for the Drell-Yan cross section. We hope the situation will improve soon.

Acknowledgments

The authors acknowledge F. Chevallier, B. Clément and Q. Li for useful discussions.

-
- [1] J. McDonald, Phys. Rev. D **50**, 3637 (1994).
 - [2] M. C. Bento, O. Bertolami and R. Rosenfeld, Phys. Lett. B **518**, 276 (2001).
 - [3] C. P. Burgess, M. Pospelov and T. ter Veldhuis, Nucl. Phys. B **619**, 709 (2001).
 - [4] H. Davoudiasl, R. Kitano, T. Li and H. Murayama, Phys. Lett. B **609**, 117 (2005).
 - [5] J. J. van der Bij, Phys. Lett. B **636**, 56 (2006).
 - [6] J. J. van der Bij and S. Dilcher, Phys. Lett. B **638**, 234 (2006).
 - [7] T. Appelquist, B. A. Dobrescu and A. R. Hopper, Phys. Rev. D **68**, 035012 (2003).
 - [8] B. Kors and P. Nath, JHEP **0507**, 069 (2005).
 - [9] W. F. Chang, J. N. Ng and J. M. S. Wu, Phys. Rev. D **74**, 095005 (2006).
 - [10] D. Feldman, Z. Liu and P. Nath, JHEP **0611**, 007 (2006).
 - [11] D. Feldman, Z. Liu and P. Nath, Phys. Rev. Lett. **97**, 021801 (2006).
 - [12] A. Ferrogli, A. Lorca and J. J. van der Bij, Annalen Phys. **16**, 563 (2007).
 - [13] C. Coriano, A. E. Faraggi and M. Guzzi, Phys. Rev. D **78** (2008) 015012.
 - [14] M. S. Chanowitz, arXiv:0806.0890 [hep-ph].
 - [15] M. S. Chanowitz, Phys. Rev. Lett. **87**, 231802 (2001).
 - [16] M. S. Chanowitz, Phys. Rev. D **66**, 073002 (2002).
 - [17] LEP electroweak working group, <http://lepewwg.web.cern.ch>.
 - [18] M. S. Carena, A. Daleo, B. A. Dobrescu and T. M. P. Tait, Phys. Rev. D **70**, 093009 (2004).
 - [19] M. Dittmar, A. S. Nicollerat and A. Djouadi, Phys. Lett. B **583**, 111 (2004).
 - [20] B. Fuks, M. Klasen, F. Ledroit, Q. Li and J. Morel, Nucl. Phys. B **797**, 322 (2008).
 - [21] A. Leike, Phys. Rept. **317**, 143 (1999).
 - [22] P. Langacker, arXiv:0801.1345 [hep-ph].
 - [23] J. C. Collins and D. E. Soper, Phys. Rev. D **16**, 2219 (1977).
 - [24] P. Langacker, R. W. Robinett and J. L. Rosner, Phys. Rev. D **30**, 1470 (1984).
 - [25] J. L. Rosner, Phys. Rev. D **54**, 1078 (1996).
 - [26] M. Dittmar, Phys. Rev. D **55**, 161 (1997).
 - [27] G. Altarelli, R. K. Ellis and G. Martinelli, Nucl. Phys. B **157**, 461 (1979).
 - [28] P. Aurenche and J. Lindfors, Nucl. Phys. B **185**, 274 (1981).
 - [29] R. Hamberg, W. L. van Neerven and T. Matsuura, Nucl. Phys. B **359**, 343 (1991) [Erratum-ibid. B **644**, 403 (2002)].
 - [30] S. Frixione and B. R. Webber, JHEP **0206**, 029 (2002).
 - [31] G. Corcella *et al.*, JHEP **0101**, 010 (2001).
 - [32] A. Ferrogli, G. Ossola and A. Sirlin, hep-ph/0406334.
 - [33] A. Ferrogli, G. Ossola and A. Sirlin, Eur. Phys. J. C **35**, 501 (2004).
 - [34] A. Ferrogli, G. Ossola, M. Passera and A. Sirlin, Phys. Rev. D **65**, 113002 (2002).
 - [35] T. Aaltonen *et al.* [CDF Collaboration], Phys. Rev. Lett. **99**, 171802 (2007).
 - [36] V. M. Abazov *et al.* [D0 Collaboration], Phys. Rev. Lett. **100**, 091802 (2008).
 - [37] D0 Collaboration, D0-NOTE 4757-CONF (March 2005); R. Gelhaus, FERMILAB-THESIS-2005-22 (August 2005).
 - [38] J. Pumplin, D. R. Stump, J. Huston, H. L. Lai, P. Nadolsky and W. K. Tung, JHEP **0207**, 012 (2002).
 - [39] ATLAS Collaboration, ATLAS-TDR-14 (1999).
 - [40] ATLAS Collaboration, ATLAS-TDR-15 (1999).
 - [41] G. L. Bayatian *et al.* [CMS Collaboration], J. Phys. G **34**, 995 (2007).